



PARAMETRIC MODEL-ORDER REDUCTION FOR VISCO-ELASTIC FINITE ELEMENT MODELS: AN APPLICATION TO MATERIAL PARAMETER IDENTIFICATION

Axel van de Walle, Elke Deckers and Wim Desmet

*Department of Mechanical Engineering, KU Leuven, Celestijnenlaan 300B, B-3001 Heverlee, Leuven, Belgium
e-mail: axel.vandewalle@kuleuven.be*

Lucie Rouleau

Structural Mechanics and Coupled Systems Laboratory, Cnam Paris, 2 Rue Conté, Paris, France

In many engineering applications, viscoelastic treatments are used to suppress vibrations of lightly damped structures. The most commonly used method to model the dynamics of complex structures is the finite element method. Its use, however, often results in very large and computationally demanding models. To alleviate this problem, model-order reduction (MOR) techniques have been developed to reduce the size of the finite element model while still maintaining an accurate description of the most important system dynamics. In order to apply these MOR schemes, the parameter values of the full-order model (including viscoelastic material properties) have to be fixed. Recently though, parametric model-order reduction (pMOR) techniques have been introduced, allowing the parameter dependency to be retained in the reduced-order models. This makes them a valuable tool for use in optimization procedures. This paper presents a Krylov subspace technique for reduced-order modelling, embedded in a recent pMOR framework. The viscoelastic material properties are modelled using the Golla-Hughes-McTavish formulation. This procedure is then applied to a finite element model of a cantilever beam with viscoelastic treatment. The resulting reduced-order model is used to identify viscoelastic material properties from experiments through an inverse optimization procedure, demonstrating both the efficiency and accuracy of the obtained reduced-order model.

1. Introduction

The finite element (FE) method is one of the most important and widespread numerical tools for the dynamic analysis of elastic engineering structures. Various formulations for the modelling of viscoelastic damping materials exist, and some of these have been successfully integrated into FE models, e.g. in [1]. However, the numerical models resulting from FE-discretization are often very large in size, resulting in long computation times.

The use of model-order reduction (MOR) techniques can drastically reduce the model size and associated computational burden. There have been previous attempts to apply MOR-techniques to finite element models incorporating viscoelastic materials. A component mode synthesis (CMS) approach is paired to a fractional derivative model for viscoelasticity in [2]. Salmanoff uses balanced

truncation (BT) with Golla-Hughes-McTavish (GHM) models for viscoelasticity in [3]. The cost of solving the associated Lyapunov equations scales badly with model size, which limits the practical applicability of BT to small models. Zghal et al. investigate the application of dynamic, Guyan and modal reductions to GHM models in [4], but the performance of these methods is moderate. In [5], proper orthogonal decomposition (POD) is successfully used to reduce the order of a model containing a Maxwell formulation for viscoelasticity. The POD procedure needs snapshots to be generated for the construction of the projection base. This requires multiple simulations to be carried out using the full-order model (FOM), which results in a large computational cost.

With the exception of [5], all of the works mentioned above do not allow the viscoelastic material parameters to change in the reduced-order model (ROM). This paper presents a parametric MOR (pMOR) technique for the reduced-order modelling of viscoelastic materials, based on a Krylov subspace reduction [6]. Since most MOR methods do not handle frequency-dependent system matrices well, a GHM formulation is used to model the viscoelastic material behaviour.

2. GHM method for modelling viscoelastic finite elements

Viscoelastic material behaviour can be modelled by using a complex and frequency-dependent material modulus. For the GHM method [7], the following expression represents this modulus in the Lapace domain:

$$(1) \quad G(s) = \sum_{k=1}^m G_k^0 + h_k(s) = \sum_{k=1}^m G_k^0 + \frac{\alpha_k s^2 + \alpha_k \beta_k s}{s^2 + \beta_k s + \delta_k},$$

with m the number of mini-oscillator terms. Assuming that all G_k^0 are known and fixed, this leads to a set of 3 parameters $\{\alpha_k, \beta_k, \delta_k\}$ for each mini-oscillator term.

The GHM method allows to express the governing system of equations using only frequency-independent FE matrices. The GHM viscoelastic element matrices M_v^{el} , C_v^{el} and K_v^{el} have the following structure:

$$(2) \quad M_v^{el} = \begin{bmatrix} M_e^{el} & 0 & \cdots & 0 & 0 \\ 0 & \frac{\alpha_1}{\delta_1} \Lambda_1 & 0 & \cdots & 0 \\ \vdots & 0 & \ddots & 0 & \vdots \\ 0 & \vdots & 0 & \frac{\alpha_k}{\delta_k} \Lambda_k & 0 \\ 0 & 0 & \cdots & 0 & \ddots \end{bmatrix}, \quad C_v^{el} = \begin{bmatrix} C_e^{el} & 0 & \cdots & 0 & 0 \\ 0 & \frac{\alpha_1 \beta_1}{\delta_1} \Lambda_1 & 0 & \cdots & 0 \\ \vdots & 0 & \ddots & 0 & \vdots \\ 0 & \vdots & 0 & \frac{\alpha_k \beta_k}{\delta_k} \Lambda_k & 0 \\ 0 & 0 & \cdots & 0 & \ddots \end{bmatrix},$$

$$K_v^{el} = \begin{bmatrix} K_e^{el} (1 + \sum \alpha_k) & -\alpha_1 R_1 & \cdots & -\alpha_k R_k & \cdots \\ -\alpha_1 R_1^T & \alpha_1 \Lambda_1 & 0 & \cdots & 0 \\ \vdots & 0 & \ddots & 0 & \vdots \\ -\alpha_k R_k^T & \vdots & 0 & \alpha_k \Lambda_k & 0 \\ \vdots & 0 & \cdots & 0 & \ddots \end{bmatrix},$$

with M_e^{el} , C_e^{el} and K_e^{el} the elastic element matrices. The matrices R_k and Λ_k originate from the eigenvalue decomposition of the G_k^0 modulus-factored stiffness matrix K_e^{el} . These viscoelastic element matrices can be split into parameter-dependent and parameter-independent parts:

$$\begin{aligned}
(3) \quad M_v^{el} &= M_{ve}^{el} + \sum \frac{\alpha_k}{\delta_k} M_{vp,k}^{el}, \\
C_v^{el} &= C_{ve}^{el} + \sum \frac{\alpha_k \beta_k}{\delta_k} C_{vp,k}^{el}, \\
K_v^{el} &= K_{ve}^{el} + \sum \alpha_k K_{vp,k}^{el}.
\end{aligned}$$

After assembly, the global system matrices can be decomposed in a similar way:

$$\begin{aligned}
(4) \quad M &= M_e + \sum \frac{\alpha_k}{\delta_k} M_{p,k}, \\
C &= C_e + \sum \frac{\alpha_k \beta_k}{\delta_k} C_{p,k}, \\
K &= K_e + \sum \alpha_k K_{p,k}.
\end{aligned}$$

These matrices are frequency-independent. The Laplace-domain representation of the system dynamics is now

$$(5) \quad [s^2 M + sC + K]X(s) = F(s),$$

which exhibits the same structure and matrix properties as a regular elastic FE model [7].

3. Parametric model-order reduction for GHM models

3.1 Parametric model-order reduction

Common MOR methods (such as CMS, Krylov subspace reduction, BT, ...) strive to find a suitable projection matrix pair $\{W, V\}$ to reduce the number of degrees of freedom (DOFs) while maintaining a high level of accuracy. Unfortunately most of these methods do not cope well with frequency-dependent system matrices, and only provide an accurate model description for a single, fixed set of parameter values. With the GHM method described in section 2 it is possible to obtain a set of frequency-independent system matrices at the expense of introducing additional DOFs. This increase in DOFs is of little concern since MOR methods can now be applied to reduce the model order.

The importance of parametric studies has led to the development of parametric model-order reduction techniques that are able to preserve the parameter dependency of the original FE model in the reduced-order model. This work adopts a Krylov subspace reduction technique, embedded in the pMOR approach developed by Baur et al. in [8], to obtain highly accurate, frequency-independent and parametrized reduced-order models of viscoelastic structures.

3.2 Application to GHM models

The pMOR procedure described above is used to find a suitable projection matrix pair $\{W, V\}$. The reduced system of equations is obtained by projecting the system of equations in eq. (5) onto this matrix pair:

$$(6) \quad [s^2 M_r + sC_r + K_r]\hat{X}(s) = F_r(s),$$

with

$$(7) \quad \begin{aligned} X(s) &= V \hat{X}(s), \\ F_r(s) &= W^T F(s), \end{aligned}$$

and

$$(8) \quad \begin{aligned} M_r &= W^T M V = W^T M_e V + \sum \frac{\alpha_k}{\delta_k} W^T M_{p,k} V = M_{e,r} + \sum \frac{\alpha_k}{\delta_k} M_{p,k,r}, \\ C_r &= W^T C V = W^T C_e V + \sum \frac{\alpha_k \beta_k}{\delta_k} W^T C_{p,k} V = C_{e,r} + \sum \frac{\alpha_k \beta_k}{\delta_k} C_{p,k,r}, \\ K_r &= W^T K V = W^T K_e V + \sum \alpha_k W^T K_{p,k} V = K_{e,r} + \sum \alpha_k K_{p,k,r}. \end{aligned}$$

The reduced system matrices in eq. (8) have the same parameter structure as the full-order system matrices in eq. (4). Therefore, when using this pMOR method, the calculation of the system response and the gradients of the system response w.r.t. the GHM parameters for the ROM can be performed in the same way as for the FOM.

3.3 Numerical experiment: a clamped viscoelastic cantilever beam

To illustrate the accuracy of the method described in section 3.2, the application to a FE model of a viscoelastic cantilever beam is presented in this section. The beam is modelled using 120 beam elements, and is loaded by a point force at the free end. For the sake of simplicity and to be able to visualize the numerical results, only one mini-oscillator term is considered, such that the model includes three viscoelastic material parameters: α , β and δ . The complex material modulus is now described by

$$(9) \quad G(s) = G^0 + h(s) = G^0 + \frac{\alpha s^2 + \alpha \beta s}{s^2 + \beta s + \delta}.$$

The transverse acceleration at the free end in response to a unit force is calculated using both the FOM and the parametric ROM (pROM) to evaluate the reduction error. The relative reduction error is defined as

$$(10) \quad \varepsilon_{rel}(\omega) = \frac{|A_{FOM}(\omega) - A_{pROM}(\omega)|}{|A_{FOM}(\omega)|},$$

with A the transverse acceleration at the free end. Figure 1 depicts the ∞ -norm of the relative reduction error in the frequency range 0-500 Hz using isosurfaces. The blue circles represent the points in the parameter space that were used in the construction of the pROM. The reduction error is very small over a broad range of parameter values, and only becomes significant near the parameter point $\{1, 10, 10^7\}$. The model size was reduced from 480 DOFs for the FOM to 32 DOFs for the pROM.

4. Viscoelastic material parameter identification

This section presents an optimization-based material parameter identification as a case study to illustrate the advantage of pMOR in parametric studies for viscoelastic structures. The model that is used in this identification procedure is the beam model presented in section 3.3. The objective is to identify the viscoelastic material parameters $\{\alpha, \beta, \delta\}$ from an experimental frequency response function.

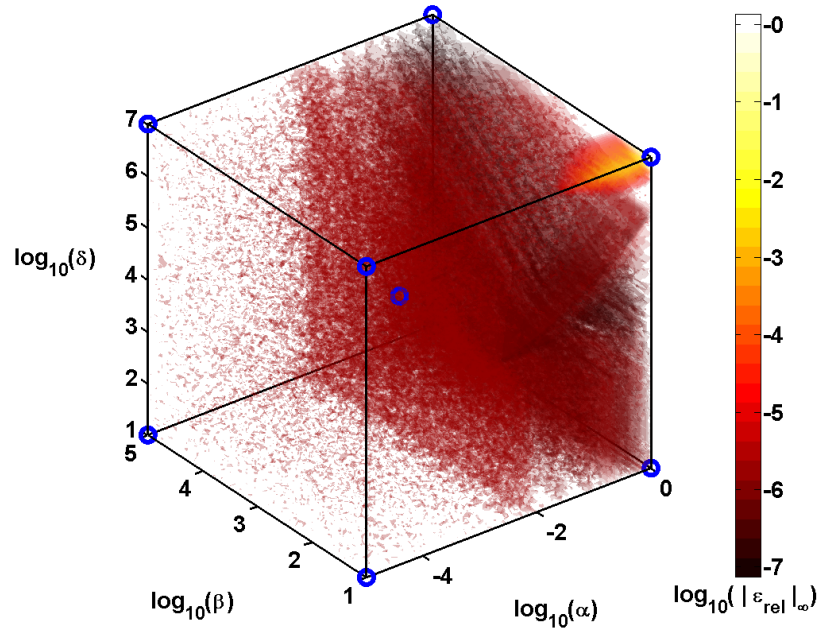


Figure 1: The ∞ -norm of the relative reduction error in the frequency range 0-500 Hz is sufficiently small over the considered parameter space.

4.1 Identification procedure

The set of viscoelastic material parameters $\{\alpha, \beta, \delta\}$ can be identified by minimizing the difference between an obtained experimental response and the theoretical response predicted by a numerical model containing these parameters. The parameter set $\{\alpha, \beta, \delta\}$ which yields the smallest difference between both responses is the best set to represent the viscoelastic behaviour. The identification procedure can therefore be expressed as the following minimization problem:

$$(11) \quad \arg \min_{\log_{10}(\alpha), \log_{10}(\beta), \log_{10}(\delta)} \log_{10} \left(\sum_{l=1}^{n_{freq}} (T_{exp}^l - T_{num}^l)^2 \right),$$

with T_{\bullet}^l defined as:

$$(12) \quad T_{\bullet}^l = 20 \log_{10} \left(\left| \frac{A_{\bullet}(\omega_l)}{F_{\bullet}(\omega_l)} \right| \right),$$

where A_{\bullet} is the transverse acceleration and F_{\bullet} the force input. The variable n_{freq} indicates the number of frequencies at which the system response is evaluated. It is possible to use a different cost function to quantify the discrepancy between the experimental and numerical responses, but expression (11) provides a relatively smooth and well-conditioned cost function. The choice to optimize w.r.t. $\{\log_{10}(\alpha), \log_{10}(\beta), \log_{10}(\delta)\}$ instead of $\{\alpha, \beta, \delta\}$ is made to efficiently cover a broad range of parameter values.

The algorithm that is used for the optimization is a combined BFGS - steepest descent method, coupled to an Armijo line search algorithm, and is quite similar to the method used in [9]. The BFGS method needs the (estimated) Hessian of the cost function to be positive definite. Since the cost function is non-convex in a considerable part of the parameter space, BFGS can often not be used throughout the whole optimization procedure. When a non-positive definite Hessian is detected, a

steepest descent step is performed instead. This mixed algorithm is both efficient and robust, but it should be noted that the risk of converging to a local optimum is still present. If required, the current optimization algorithm can be embedded into a simulated annealing or a multiple starting point procedure to transform it into a global optimization method.

4.2 Numerical experiments

The numerical experiments in this section perform the identification procedure outlined in section 4.1 using both the FOM and pROM of the viscoelastic cantilever beam described in section 3.3. The experimental response is generated in a simulated experiment using the FOM in a design parameter point $\{\log_{10}(\alpha_d), \log_{10}(\beta_d), \log_{10}(\delta_d)\}$. The optimization results obtained using the FOM serve as a benchmark to assess the performance of the pROM.

4.2.1 Two-parameter identification

In the first experiment, the value of the parameter α is fixed, while the optimization procedure is used to identify the values of the parameters β and γ . The design parameter point is located at $\{-1, 4, 6\}$. Table 1 summarizes the most important results of the optimization procedure for different initial parameter points. Both the FOM and the pROM converge well onto the design parameter point. The advantage of using pMOR is illustrated by the speedup factor: for this example, the pMOR technique speeds up calculations by a factor of about 8. The speedup will be even more substantial for larger and more complex FE models. The initial and optimized numerical responses for case a, as well as the frequency points at which the cost function in expression (11) is evaluated, are shown in figure 2. Figure 3 depicts the consecutive points in the parameter space chosen by the optimization procedure. The dots represent the points chosen using the pROM, while the crosses indicate the path followed using the FOM. Figure 3 shows that the optimization paths are very similar, and that the cost function defined in expression (11) is sufficiently smooth.

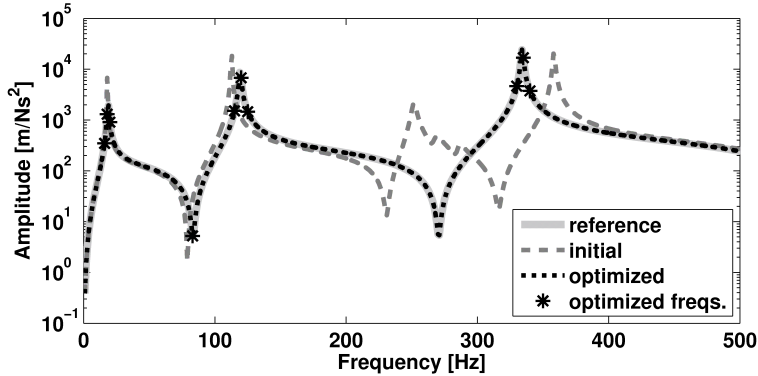


Figure 2: Responses in p_{design} , p_{init} and $p_{opt,pROM}$ for case a.

Table 1: Numerical results of the optimization in two parameters.

case	p_{init}	$p_{opt,FOM}$	$p_{opt,pROM}$	$n_{it,FOM}$	$n_{it,pROM}$	speedup
a	$\{-1, 1.5, 6.5\}$	$\{-1, 4.0000, 6.0000\}$	$\{-1, 4.0000, 6.0000\}$	41	41	8.1
b	$\{-1, 1.1, 4.2\}$	$\{-1, 4.0000, 6.0000\}$	$\{-1, 4.0000, 6.0000\}$	40	42	7.5
c	$\{-1, 5, 4\}$	$\{-1, 4.0000, 6.0000\}$	$\{-1, 4.0000, 6.0000\}$	35	35	8.1
d	$\{-1, 3.75, 7\}$	$\{-1, 4.0000, 6.0000\}$	$\{-1, 4.0000, 6.0000\}$	31	31	8.0

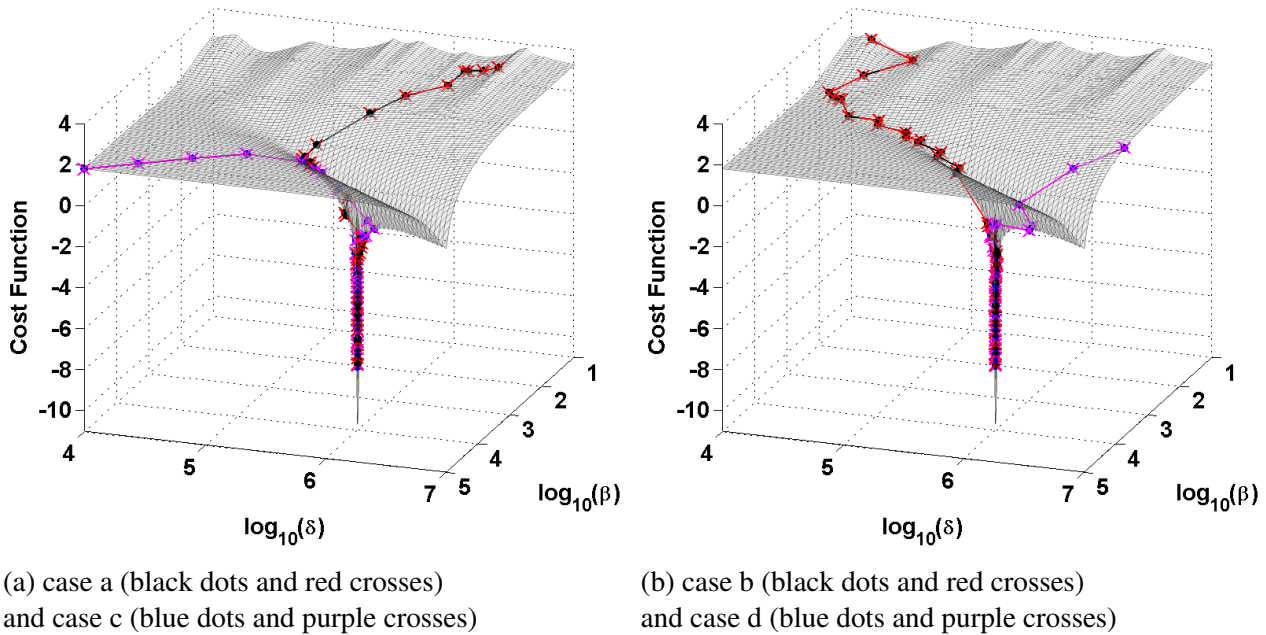


Figure 3: Cost function and optimization paths in the β - δ parameter space. Dots represent the path followed using the pROM, while crosses represent the path obtained using the FOM.

4.2.2 Three-parameter identification

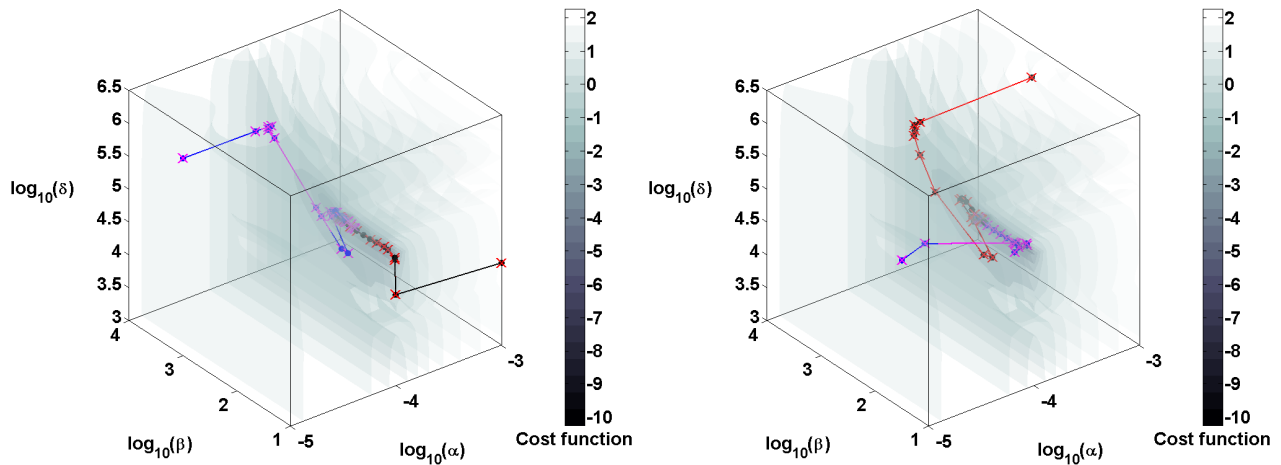
In the second experiment, all three material parameters $\{\alpha, \beta, \delta\}$ are now identified using the optimization procedure. The design parameter point is located at $\{-4, 2, 5\}$. Table 2 shows that the FOM can be replaced by the pROM without significant loss of accuracy, while resulting in a reduction of computational effort. Figure 4 visualizes the cost function (using surfaces of constant cost value) and optimization paths in the parameter space. The optimization paths obtained using the FOM and the pROM are again very similar.

Table 2: Numerical results of the optimization in three parameters.

case	P_{init}	$P_{opt,FOM}$	$P_{opt,pROM}$	$n_{it,FOM}$	$n_{it,pROM}$	speedup
e	$\{-3, 1, 4.25\}$	$\{-3.9999, 1.9951, 4.9988\}$	$\{-3.9999, 1.9993, 4.9995\}$	21	24	7.0
f	$\{-3, 3, 6\}$	$\{-4.0001, 2.0054, 5.0014\}$	$\{-4.0000, 2.0000, 4.9995\}$	26	28	7.7
g	$\{-5, 3, 6\}$	$\{-3.9999, 1.9961, 4.9990\}$	$\{-4.0001, 2.0038, 5.0004\}$	30	30	8.4
h	$\{-5, 1.5, 4.25\}$	$\{-4.0001, 1.9961, 4.9997\}$	$\{-4.0001, 2.0074, 5.0015\}$	29	25	7.2

5. Conclusion

This paper presents a method for the construction of accurate, frequency-independent and parametrized reduced-order finite element models of viscoelastic structures. Combining the frequency-independent Golla-Hughes-McTavish formulation for viscoelastic finite elements with Krylov subspace methods for model-order reduction leads to a streamlined process for obtaining compact yet accurate models of viscoelastic structures. By embedding this process in a parametric model-order reduction framework, fast evaluations of the system response for varying viscoelastic parameters can be obtained. The benefits of the proposed method are demonstrated for an optimization-based viscoelastic material parameter identification.



(a) case e (black dots and red crosses)
and case g (blue dots and purple crosses)

(b) case f (black dots and red crosses)
and case h (blue dots and purple crosses)

Figure 4: Cost function and optimization paths in the α - β - δ parameter space. Dots represent the path followed using the pROM, while crosses represent the path obtained using the FOM.

Acknowledgements

The research of Axel van de Walle is funded by a Ph.D. Grant of the Agency for Innovation by Science and Technology in Flanders (IWT). The Fund for Scientific Research - Flanders (F.W.O.) is gratefully acknowledged for the support of the postdoctoral research of Elke Deckers. The authors also gratefully acknowledge the European Commission for their support through the research project GA-285808 INTERACTIVE.

REFERENCES

- de Lima, A.M.G., Stoppa, M.H. and Rade, D.A. Finite element modeling of structures incorporating viscoelastic materials, *Proceedings of the 21st IMAC Conference and Exposition (IMAC XXI)*, Kissimmee, Florida, 3–6 February, (2003).
- Rouleau, L., Deü, J.-F., Legay, A., Sigrist, J.-F., Le Lay, F. and Marin-Curtoud, P. A component mode synthesis approach for dynamic analysis of viscoelastically damped structures, *Proceedings of the 10th World Congress on Computational Mechanics*, Sao Paulo, Brazil, 8–13 July, (2012).
- Salmanoff, J., *A Finite Element, Reduced Order, Frequency Dependent Model of Viscoelastic Damping*, PhD Thesis, Virginia Polytechnic Institute and State University, (1997).
- Zghal, S., Bouazizi, M.L., Bouhaddi, N. and Nasri, R. Model reduction methods for viscoelastic sandwich structures in frequency and time domains, *Finite Elements in Analysis and Design*, **93**, 12–29, (2015).
- Brigham, J.C. and Aquino, W. Inverse viscoelastic material characterization using POD reduced-order modeling in acoustic-structure interaction, *Computer Methods in Applied Mechanics and Engineering*, **198**, 893–903, (2009).
- Grimme, E. J., *Krylov projection methods for model reduction*, PhD Thesis, ECE Department, University of Illinois, (1997).
- Golla, D.F., and Hughes, P.C. Dynamics of Viscoelastic Structures - A Time-Domain, Finite Element Formulation, *Journal of Applied Mechanics*, **52**, 897–906, (1985).
- Baur, U., Beattie, C., Benner, P., Gugercin, S. Interpolatory projection methods for parameterized model reduction, *SIAM J. Sci. Comput.*, **33** (5), 2489–2518, (2011).
- Rouleau, P., Pluymers, B. and Desmet, W. Characterisation of viscoelastic layers in sandwich lightweight panels through inverse techniques, *Proceedings of the international congress on noise and vibration: emerging methods (NOVEM2015)*, Dubrovnik, Croatia, 13–15 April, (2015).